

# Mapping of Mount Semeru Volcanic Mudflow Susceptibility Along the Rejali River using the GIS-based AHP-TOPSIS Ensemble Approach

Sonia Oktariyanti<sup>1</sup>, Entin Hidayah<sup>1,\*</sup>, Saifurridza<sup>1</sup>, Mokhammad Farid Ma'ruf<sup>1</sup>,  
Nunung Nuring Hayati<sup>1</sup>, Zulkifli Yusop<sup>2</sup>

<sup>1</sup>Department of Civil Engineering, University of Jember, Jember, INDONESIA  
Jalan Kalimantan Tegalboto No 37, East Krajan, Sumbersari, Jember

<sup>2</sup>Civil Engineering Department, Centre for Sustainable Environment and Water Security,  
Universiti Teknologi Malaysia, Johor, MALAYSIA

\*Corresponding author: [entin.teknik@unej.ac.id](mailto:entin.teknik@unej.ac.id)

SUBMITTED 08 January 2023   REVISED 17 May 2023   ACCEPTED 22 May 2023

**ABSTRACT** Volcanic mudflow floods occur when rainfall runoff combines with volcanic material and flows downstream. These devastating events cause significant damage to infrastructure, disrupt economies, and result in injuries and casualties. One area where the flow of volcanic material greatly affects the situation is the Rejali River, which receives a substantial amount of volcanic debris from Mount Semeru. To address this issue and begin mitigating the associated risks, it is crucial to start by mapping the potential distribution of volcanic mudflow floods. Therefore, this study aimed to assess factors impacting volcanic mudflow flood susceptibility and to create a corresponding susceptibility map. The study employed the Analytical Hierarchy Process (AHP) and the Technique for Order Preference by Similarity to Ideal Solution (TOPSIS) to determine the influence of various factors and classify the areas, respectively. These methods were integrated with the Geographic Information System (GIS) to enhance the analysis. The weighted analysis results showed that the most impactful factors conditioning volcanic mudflow floods, in descending order, were rainfall (42.40%), land cover (13.89%), elevation (13.39%), slope (12.51%), distance from the river (7.09%), soil type (6.58%), and rock distribution (4.13%). The TOPSIS calculation further highlighted that rainfall intensity between 104.03 and 109.65 mm day<sup>-1</sup> had the greatest influence on susceptibility. The successful integration of AHP and TOPSIS methods with GIS helped develop a volcanic mudflow flood susceptibility model with an outstanding accuracy of 0.969. The model showed that approximately 46.40% of the areas along the Rejali River exhibited very high susceptibility to volcanic mudflow floods, while an additional 16.21% indicated high susceptibility and substantial risk in most regions. Therefore, the generated susceptibility map offered important insights for shaping future mitigation strategies and influencing policy decisions.

**KEYWORDS** Mitigation; Model Accuracy; Flood; Volcanic Mudflow; Risk Mapping

© The Author(s) 2023. This article is distributed under a Creative Commons Attribution-ShareAlike 4.0 International license.

## 1 INTRODUCTION

Semeru Mountain, a notable volcano in Indonesia, is a significant threat due to its frequent eruptions. These eruptions produce vast quantities of volcanic material, potentially triggering mudflow flood during heavy rainfall. Furthermore, the Meteorology, Climatology, and Geophysics Agency (BMKG) has recently issued an extreme weather alert. This alert amplifies the potential for catastrophic mudflow flood in the Semeru area, specifically in the hard-hit Rejali watershed. Mitigation of potential losses necessitates the development of a mudflow flood susceptibility map. This map serves as a critical tool, providing vital information about potential volcanic mudflow flood distribution in the area (Armijon et al., 2018).

Hydrological and hydraulic modeling software, such as HEC-HMS and HEC-RAS, are widely used for detailed analyses of volcanic mudflow flood susceptibility (Akay, 2021). However, using Geographic Information System (GIS)-based methods to identify volcanic mudflow flood susceptibility is a novel and challenging approach. GIS simplifies this process by incorporating various flood-related factors in an overlay method (Meydani et al., 2022). It also utilizes high-resolution topographic data, hence ideal for modeling flood susceptibility (Irawan et al., 2019). A distinct modeling approach focuses on geomorphological factors like rainfall intensity, slope, elevation, soil type, rock distribution, land cover, and river dis-

tance (Costache et al., 2020; Ulfiana, 2020; Ulfiana and Sari, 2020). These seven factors influence volcanic mudflow flood occurrence, but their significance varies by location.

Various statistical and multicriteria models, such as frequency ratio (FR), weight of evidence (WoE), fuzzy logic (FL), evidential belief function (EBF), index of entropy (IoE), analytical hierarchy process (AHP), principal component analysis (PCA), technique for order preference by similarity to an ideal solution (TOPSIS), and VIKOR have been used to model volcanic mudflow flood susceptibility (Khosravi et al., 2019). AHP is considered simple yet effective for handling multiple factors. However, it requires expert judgment, which can introduce bias and potentially lower accuracy, forming its limitations (Nyimbili et al., 2018).

To address this concern, the use of an ensemble approach combining the Analytic Hierarchy Process (AHP) with other methods is crucial (Ulfiana, 2020; Ulfiana and Sari, 2020). One such successful application of this approach is the AHP-TOPSIS method, which enables accurate prediction of flood susceptibility (Tabarestani and Afzalimehr 2021).

## 2 STUDY LOCATION

This study was conducted on the Rejali River Basin in the Mount Semeru area, spanning approximately 13,094.06 hectares based on the author's geographic information system analysis. According to Safitri et al. (2021), this geographical location was situated at 8° 06' 30" S latitude and 112° 55' E longitude, as shown in Figure 1. The highest elevation in this area, as per the Digital Elevation Model (DEM) data, was 3609.27 m above sea level. The Rejali watershed upper reaches were located in the Mount Semeru area, extending through the Perak Sumberwuluh Deck and ending in Jugosari Village, Candipuro District. The selection of this location stems from its historical relevance, particularly the volcanic mudflow flood that ensued on December 4, 2021, following the eruption of Mount Semeru (Oktavia et al., 2022).

## 3 METHODS

The study on volcanic mudflow flood susceptibility is divided into four stages, as shown in Figure

2. The first stage was creating and classifying a map of volcanic mudflow flood susceptibility factors for the TOPSIS process. The second involved calculating the weight of each volcanic mudflow flood susceptibility factor from the respondents' interviews using the AHP process. The third stage involved mapping volcanic mudflow flood susceptibility with the AHP-TOPSIS method. The final stage validated this model using an area under the curve (AUC) value based on a Disaster-Prone Area map, which served as a volcanic mudflow flood inventory.

### 3.1 Selection of volcanic mudflow flood factors

This study used seven key factors influencing volcanic mudflow flood susceptibility to create the initial map, all of which had been previously identified as having significant impact on such events (Ulfiana, 2020). Specifically, these factors included DEMNAS data (elevation and slope), Digital Topography Map (BIG 2019) (land use, soil type, river distance, and rock distribution), rainfall intensity data, and volcanic mudflow flood inventory data, as shown in Table 1. The final data processing step was to convert the data into raster format to standardize the resolution. The natural breaks method was then used to categorize elevation and rainfall into five classes (Akay, 2021). Other factors such as slope, land use, soil type, river distance, and rock distribution were classified based on established regulations (Darmawan et al., 2017). These classifications facilitated the interpretation of the susceptibility level (Seejata et al., 2018).

The elevation factor, indicating the vertical distance of an area from sea level, was inversely related to volcanic mudflow flood probability. Areas with higher elevations had lower flood probabilities (Khosravi et al., 2018). As shown in Figure 3(a), the classified elevation map revealed varied ranges: 46.37% of the land was between 0 and 292 m; 28.49% between 292 and 617 m; 17.05% between 617 and 1153 m; 5.84% between 1153 and 2028 m; and 2.25% above 2028 m.

The slope factor, the ratio of horizontal to vertical distance, significantly impacted runoff (Purnawali, 2018). Figure 3(b) displayed the slope map of the Rejali watershed, derived from DEMNAS data processing. This classification underscored that 44.22% of the terrain had slopes be-

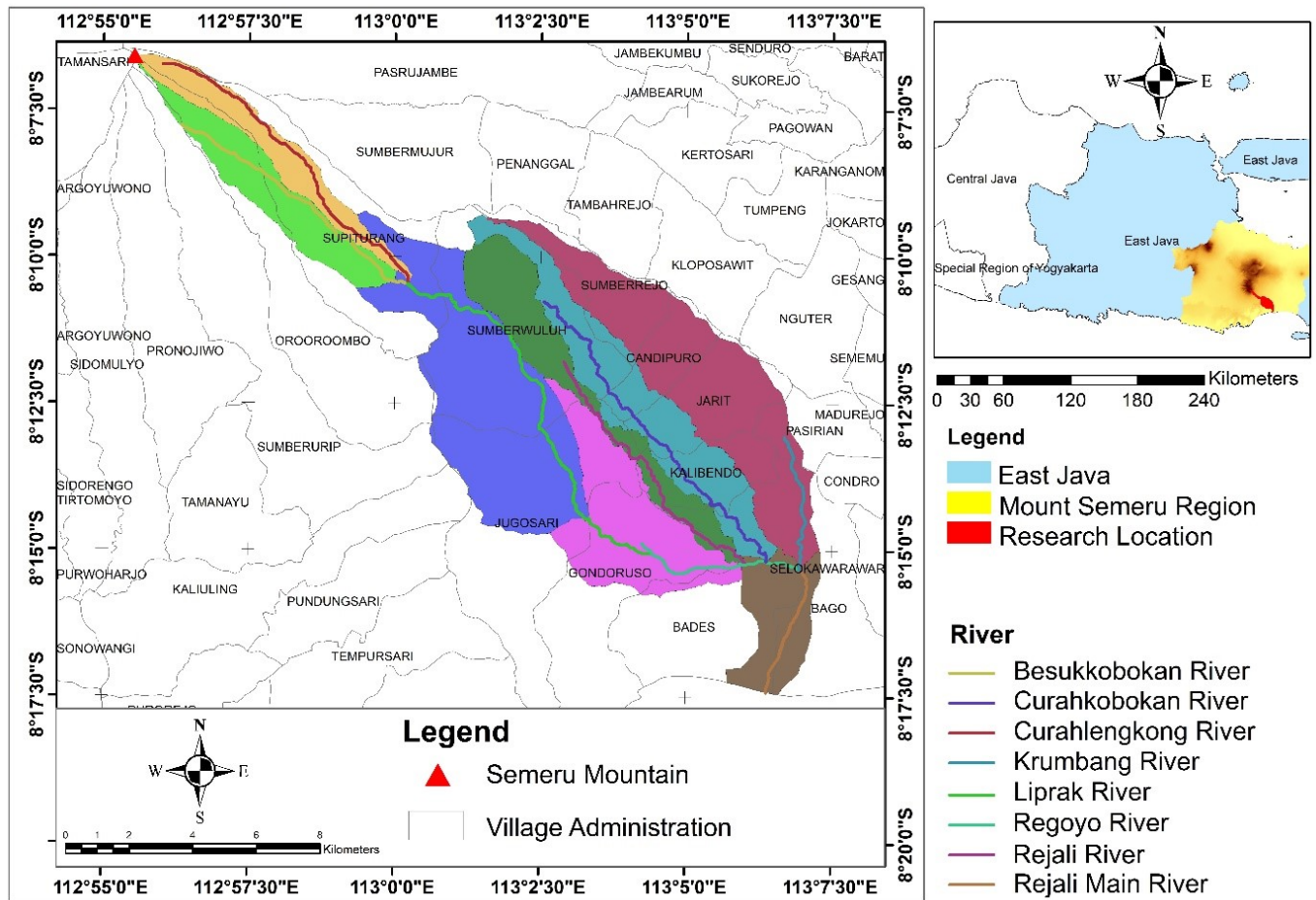


Figure 1 Location of Rejali River

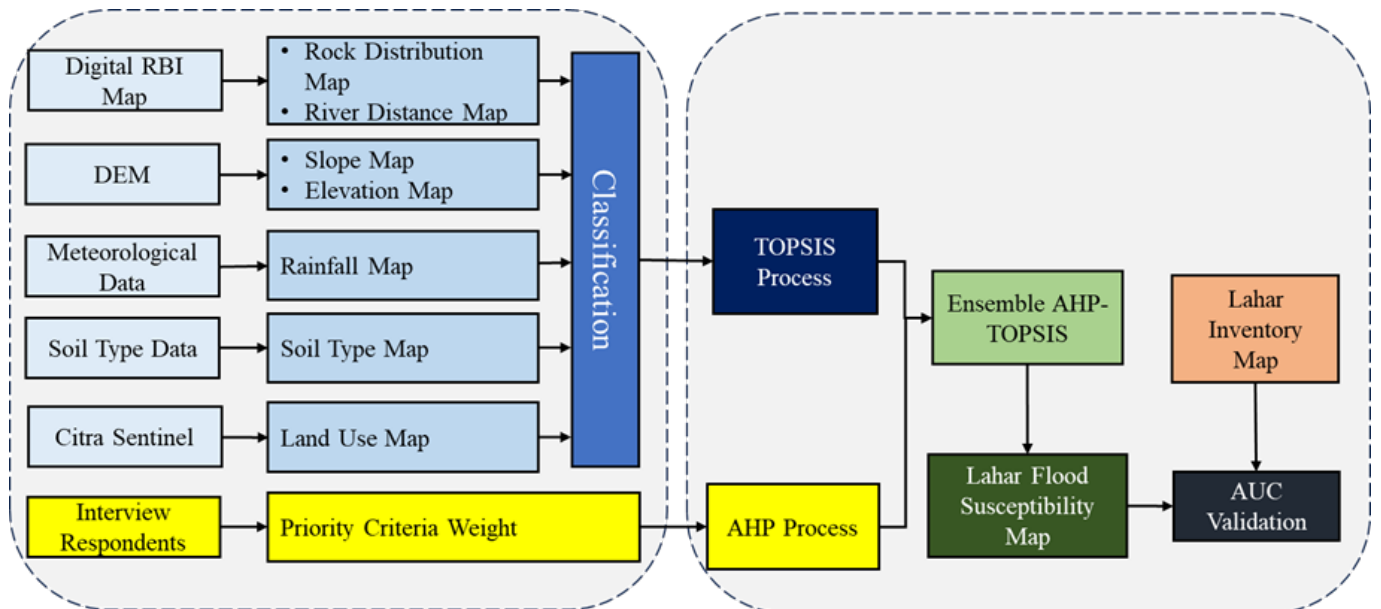


Figure 2 Flowchart of stages

tween 0 and 8%; 22.81% between 8 and 15%; 8.56% between 15 and 25%; 13.30% between 25 and 45%; and 11.11% had slopes over 45%. These

statistics classified the Rejali watershed as a ramp, highlighting its vulnerability to volcanic mudflow floods.

Table 1. Data types and sources for volcanic mudflow flood susceptibility factors

No	Data Type	Source	Information
1.	Elevation	DEMNAS	Resolution 8 m
2.	Slope	<a href="https://tanahair.indonesia.go.id/demnas/#/demnas">https://tanahair.indonesia.go.id/demnas/#/demnas</a>	
3.	Land Use	RBI BIG 2019	Scale 1:25,000
4.	Type of Soil		
5.	Distance to River	<a href="https://tanahair.indonesia.go.id/portal-web/download/perwilayah">https://tanahair.indonesia.go.id/portal-web/download/perwilayah</a>	
6.	Rock Distribution		
7.	Rainfall	Water Resources Management Unit of Lumajang Regency	Ten years (2012-2021)
8.	Volcanic Mudflow Flood Inventory	Meteorology, Climatology, and Geophysics Agency <a href="https://magma.esdm.go.id/v1/gunung-api/peta-kawasan-rawan-bencana">https://magma.esdm.go.id/v1/gunung-api/peta-kawasan-rawan-bencana</a>	Resolution 8 m

Land use, which represents how living beings utilize their surroundings to meet their needs, played a crucial role in this analysis (Pratiwi, 2020). Figure 3(c) presents the land use map of the Rejali watershed, derived from the RBI map, providing valuable insights. The map indicated that the composition of land use in the area consisted of 31.77% forest, 36.07% rice fields, 16.97% grasslands, 4.54% settlements, 1.46% vacant land, and 9.19% sand. The dominant land uses were rice fields and forests.

The infiltration process was notably affected by soil type, with higher soil moisture leading to reduced infiltration rates (Budiarti et al., 2018). Figure 3(d) presents the soil type map of the Rejali watershed, derived from the RBI map, revealing insightful information. The map indicated that the area consisted of 17.05% andosol soil, 6.65% alluvial soil, 56.46% mediterranean soil, and 19.83% grumusol soil. The predominant soil type in the region was mediterranean soil.

The factor of river distance, which gauged how close an area was to a river, suggested that shorter distances increased volcanic mudflow flood risks. (Saputra et al., 2020). The river distance map, derived from the Indonesian Earth Map and processed with the Buffer tool in ArcMap software, was shown in Figure 3(e). It showed that 0.20% of areas were within 0 to 3 m from the river, 10.79% were within 3 to 168 m, 9.07% within 168 to 333 m, 8.47% within 333 to 500 m, and a substantial 71.46% more than 500 m away.

The rock distribution factor, referring to a mineral's resistance to abrasion or susceptibility to being scratched, also affected flooding potential (Larasati, 2017). The rock distribution map classification in Figure 3(f) reported 0.60% alluvial,

0.15% breakthrough rocks, 0.71% Mount Kepolo Parasite Deposits, a significant 79.35% Mount Semeru Parasite Deposits, 0.19% Mandalika formations, 16.57% Mount Semeru parasite lava, and 2.42% Mount Kepolo parasite lava.

Lastly, rainfall intensity was a critical factor for volcanic mudflow flood, with higher intensities increasing flood risks (Hidayah et al., 2022). The processed rainfall data, using the IDW (Inverse Distance Weighted) Interpolation process in ArcMap software, was shown in Figure 3(g). The classification revealed 14.16% of areas within the 94.50 to 98.86 class, 18.66% within the 98.87 to 104.03 class, 28.71% within the 104.04 to 109.65 class, 22.82% within the 109.66 to 114.93 class, and 15.64% within the 114.94 to 123.76 class. The Rejali watershed predominantly experienced rainfall intensities between 104.03 and 109.65

### 3.2 Analytical Hierarchy Process (AHP) method

AHP, a decision-making method proposed by Thomas L. Saaty, incorporated multiple factors (Lappas and Kallioras, 2019). This method required expert opinions from a predetermined set of respondents. For the purposes of this study, 15 respondents with occupations relevant to river mudflow floods were carefully selected. This included 5 practitioners from the Brantas River Basin Agency (BBWS Brantas), 4 members from the Department of Public Works and Housing, and 6 from the Water Resources Management Unit of Lumajang Regency (UPT PSDA Lumajang Regency).

The respondents were tasked with assigning importance values to each factor, which ranged from 1 (least influential) to 9 (highly influential). These

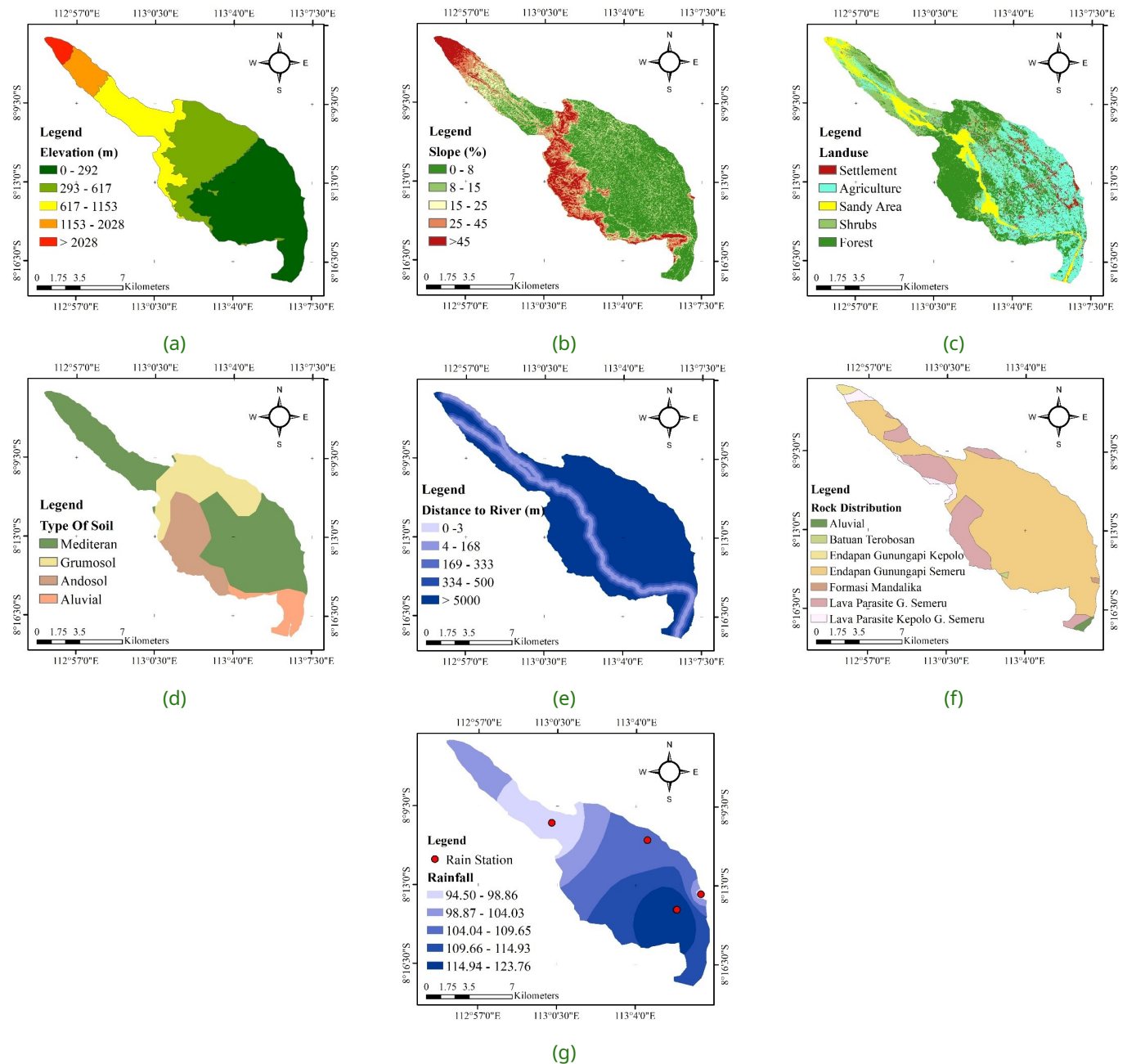


Figure 3 Classification of mudflow flood susceptibility factors (a) Elevation (b) Slope (c) Landuse (d) Type of Soil (e) Distance to river (f) Rock Distribution (g) Rainfall

values were based on their knowledge and understanding of volcanic mudflow flood susceptibility (Khosravi et al., 2018; Seejata et al., 2018).

The weight criteria were calculated using a pairwise comparison matrix measuring  $n \times n$ , derived from the respondents' comparative evaluation data. A value of one was assigned when the criteria appeared in the same row and column. A normalized matrix was then created by dividing each element by the total addition in the same column. Eigenvalues were found by dividing the

sum of the elements in each row by the number of parameters used. To ensure that the weight calculation results were consistent and suitable for use in the study, a consistency test was conducted. This was crucial, considering that the data obtained from the questionnaire were subjective (Lappas and Kallioras, 2019). For the comparison matrix to be acceptable, the consistency ratio (CR) value must be  $\leq 0.1$ . The formulas for the consistency index (CI) and CR were sequentially depicted in Equations (1) and (2).

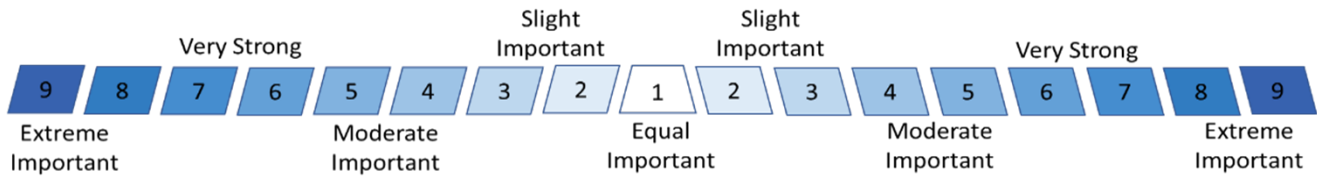


Figure 4 Hierarchical assessment importance scale  
Source: (Ulfiana and Sari, 2020)

$$CI = \frac{\lambda_{max} - n}{n - 1} \tag{1}$$

Where  $\lambda_{max}$  is the most significant value of eigenvalue and  $n$  is the multiplicity of factors used.

$$CR = \frac{CI}{RI} \tag{2}$$

Where  $CI$  is the consistency index and  $RI$  is the calculation value of Saaty in Table 2.

Table 2. Current calculation values (RI)

n	1	2	3	4	5	6	7	8	9	10
RI	0	0	0.58	0.9	1.12	1.24	1.32	1.41	1.45	1.49

### 3.2.1 Technique for Order Preference by Similarity to Ideal Solution (TOPSIS) method

TOPSIS is a method used for problem-solving. It operates on the principle that a decision should be as close as possible to the positive ideal solution and as far away as possible from the negative ideal solution. By taking into account both the positive and negative aspects of each alternative, this method offers a comprehensive evaluation. The advantage of TOPSIS is its simplicity and rationality in computation, making it an efficient tool for analysis and decision-making, particularly when dealing with multiple criteria and alternatives (Pathan et al., 2022). The steps performed in the TOPSIS method follow Equations (3) through (9) (Ching-Lai Hwang, 1981).

$$r_{ij} = \frac{x_{ij}}{\sqrt{\sum_{i=1}^m x^2}} \tag{3}$$

Where (i) and (j) are the rows and columns on the TOPSIS matrix,  $r_{ij}$  was the normalized matrix (i) (j), and  $x_{ij}$  is the decision matrix (i) (j).

$$y_{ij} = w_i r_{ij} \tag{4}$$

Where  $w_i$  is the weight of several factors (i).

$$A^+ = (y_{1+}, y_{2+}, \dots, y_{p+}) \tag{5}$$

$$A^- = (y_{1-}, y_{2-}, \dots, y_{p-}) \tag{6}$$

Where  $y_{1+}$  is the max value of  $y_{ij}$  and  $y_{1-}$  is the min value of  $y_{ij}$ .

$$D_i^+ = \sqrt{\sum_{i=1}^n (y_{ij}^+ - y_{ij})^2} \tag{7}$$

$$D_i^- = \sqrt{\sum_{i=1}^n (y_{ij} - y_{ij}^-)^2} \tag{8}$$

Where  $D_i^+$  is the distance of the  $A_i$  class with the positive ideal solution and  $D_i^-$  is the distance of the  $A_i$  class with the negative ideal solution.

$$V_i = \frac{D_i^-}{(D_i^- + D_i^+)} \tag{9}$$

### 3.2.2 Hybrid AHP-TOPSIS

The susceptibility of volcanic mudflow flood in the Rejali River was determined using the AHP-TOPSIS method. The process began by employing the Analytic Hierarchy Process (AHP) method, which involved identifying factors based on existing field conditions and a comprehensive review of prior literature studies. Once these factors were established, evaluation was conducted through interviews with a select group of respondents. This constituted a critical phase of the AHP process, as it provided an influence weight for each individual factor. The weights of the factors were then analyzed using the Technique for Order Preference

by Similarity to Ideal Solution (TOPSIS) method. The objective was to classify these factors based on their priority, effectively determining the priority class.

### 3.2.3 Insecurity Index and Validation

The AHP-TOPSIS calculation results were incorporated into each map of the volcanic mudflow flood susceptibility factors using ArcGIS. These maps were then overlaid and classified into four categories, including highly susceptible, moderately susceptible, less susceptible, and non-susceptible. The validation process employed the Area Under Curve (AUC) methodology, which compared the flood susceptibility analysis data with the volcanic mudflow flood maps obtained from the UPT PSDA Lumajang Regency. AUC values were represented graphically and range from 0.5 (imperfect) to 1 (excellent) (Hariati et al., 2018). The AUC value signified model quality, where values greater than 0.5 indicated no significant difference, those between 0.7 and 0.8 were acceptable, between 0.8 and 0.9 excellent, and 0.9 or above outstanding (Hidayah et al., 2022).

## 4 RESULTS

### 4.1 The AHP method result

The consistency test from AHP obtained a value of  $CR=0.067$ . Since it is less than 0.1, the data is consistent and feasible for this study. The most potential factor in triggering volcanic mudflow flood was rainfall, accounting for 42% of the total factor value. The rest distribution of the weighing factors was the land cover 14%, the elevation and slope 13%, the distance of rivers and soil types 7%, and the distribution of rocks 4%, as shown in Figure 6.

### 4.2 The TOPSIS method result

In this study, susceptibility levels were divided into five classes, specifically (1) very low, (2) low, (3) medium, (4) high, and (5) very high. These classifications were determined through the TOPSIS method, which distinguished the seven influencing factors into two types, benefit and cost. Factors categorized under 'benefit' implied that the higher the class of the factor, the greater its influence on volcanic mudflow flood. This included

rainfall, soil type, and rock distribution. However, the 'cost' category showed that the higher the class of the factor, the lesser its influence on volcanic mudflows. This category comprised slope, elevation, land cover, and distance from the river. Table 3 and 4 showed the AHP-TOPSIS process.

### 4.3 AHP-TOPSIS Analysis

Figure 6 showed the weight comparison of flood conditioning factors between the AHP and AHP-TOPSIS methods. The pattern remained similar, but a slight shift in weight magnitudes was observed. With the AHP-TOPSIS method, rainfall and land use factors saw minor weight increases compared to weights derived from the AHP method alone. Conversely, the weights of the other five factors (slope, elevation, soil type, river distance, and rock distribution) were slightly higher in the AHP method. This weight shift from AHP to AHP-TOPSIS was due to the values of the negative and positive factors in each area. Therefore, the TOPSIS method reduced the influence of expert judgment.

The AHP-TOPSIS method assessed the susceptibility index of volcanic mudflow floods according to their severity. The susceptibility results for the volcanic mudflow flood in the Rejali River were as follows: 6.02% of the area, or 776,166 ha, was unprotected, 22.07% or 2,847,474 ha less susceptible; 9.30% or 1,200,007 ha moderately susceptible, 16.21% or 2,090,991 ha susceptible and 46.40% or 5,986,913 ha highly susceptible. The volcanic mudflow flood susceptibility map was shown in Figure 6.

Table 5 showed the results of ten direct survey sample points carried out in the field to measure the thickness of volcanic mudflow deposits based on the flood vulnerability map. Susceptibility levels were validated according to coordinate position. Field height sampling data served as validation data for the model, describing susceptibility levels. Most surveys were conducted at high and very high susceptibility levels, with altitudes between 0.8 m and 2.8 m. From the ten data samples, a thickness of 1.5 m of volcanic mudflow was determined as the boundary between high and very high susceptibility.

Table 3. TOPSIS method results

Criterion Factors							
Class	Rainfall (mm)	Slope (%)	Elevation (m)	Soil Type	Land Use	Rock Distribution	Distance from river (m)
Classification							
1	94.5 – 98.9	0 - 8	0 - 292	Regosol, Litosol, Organosol, Renzyme	Settlement	Alluvial	0 - 3
2	98.9 – 104.0	8 - 15	292 - 617	Andosol, Grumosol	Farmland	Volcanic mudflow Parasite G semeru & G Kepolo	3 - 168
3	104.0 – 109.6	15 - 25	617 - 1153	Mediterranean Land	Sand / Vacant lots / gardens	Deposits of Parasite G semeru & G Kepolo	168 - 333
4	109.6 – 114.9	25 - 45	1153 - 2028	Latosol	Shrubs	Breakthrough Rocks	333 - 500
5	114.9 – 123.8	>45	>2028	Alluvial	Forest	Mandalika Formation	>500
Area (ha)							
	Benefit	Cost	Cost	Benefit	Cost	Benefit	Cost
1	1855	5767.28	6073.72	0	594.86	78.72	26.86
Criterion Factors							
Class	Rainfall (mm)	Slope (%)	Elevation (m)	Soil Type	Land Use	Rock Distribution	Distance from river (m)
2	2444	2975.51	3730.84	4831.09	4728.61	2489.13	1414.65
3	3760.82	1116.46	2233.43	7395.78	1395.92	10492.67	1188.96
4	2989.24	1735.08	765.24	0	2224.28	20.25	1109.96
5	2048	1449.08	294.28	871.69	4164.23	25.38	9367.02
Decision Normalization Matrix							
1	0.306	0.828	0.808	0.000	0.087	0.007	0.003
2	0.404	0.427	0.496	0.544	0.690	0.231	0.147
3	0.621	0.160	0.297	0.833	0.204	0.973	0.124
4	0.494	0.249	0.102	0.000	0.325	0.002	0.115
5	0.338	0.208	0.039	0.098	0.608	0.002	0.975
Weighted Normalization Matrix							
1	12.98	10.37	10.82	0.00	1.21	0.03	0.02
2	17.11	5.35	6.65	3.58	9.59	0.95	1.04
3	26.33	2.01	3.98	5.48	2.83	4.02	0.88
4	20.93	3.12	1.36	0.00	4.51	0.01	0.82
5	14.34	2.60	0.52	0.65	8.44	0.01	6.91
The Ideal Solution							
A+	26.33	2.01	0.52	5.48	1.21	4.02	0.02
A-	12.98	10.37	10.82	0.00	9.59	0.01	6.91

Table 4. Levels of volcanic mudflow flood susceptibility

Class	D+	D-	Preferences (V)	Susceptibility Rate
1	20.00	10.85	0.35	very low susceptible
2	14.76	10.38	0.41	low susceptible
3	3.91	20.57	0.84	medium susceptible
4	9.42	16.37	0.63	high susceptible
5	16.83	13.03	0.44	very high susceptible

4.4 Model Validation

The validation test using a model accuracy graph in very susceptible areas obtained an AUC value of

0.608 for AHP, indicating a low accuracy and was not acceptable. By using AHP-TOPSIS, the AUC value increased to 0.723 or higher than 0.7. Therefore, the AUC value was acceptable (Hidayah et al., 2022), as shown in Figure 7. The analysis results was in line with previous literature studies (Ulfiana, 2020; Ulfiana and Sari, 2020) which established that rainfall is a significant factor in flood susceptibility.

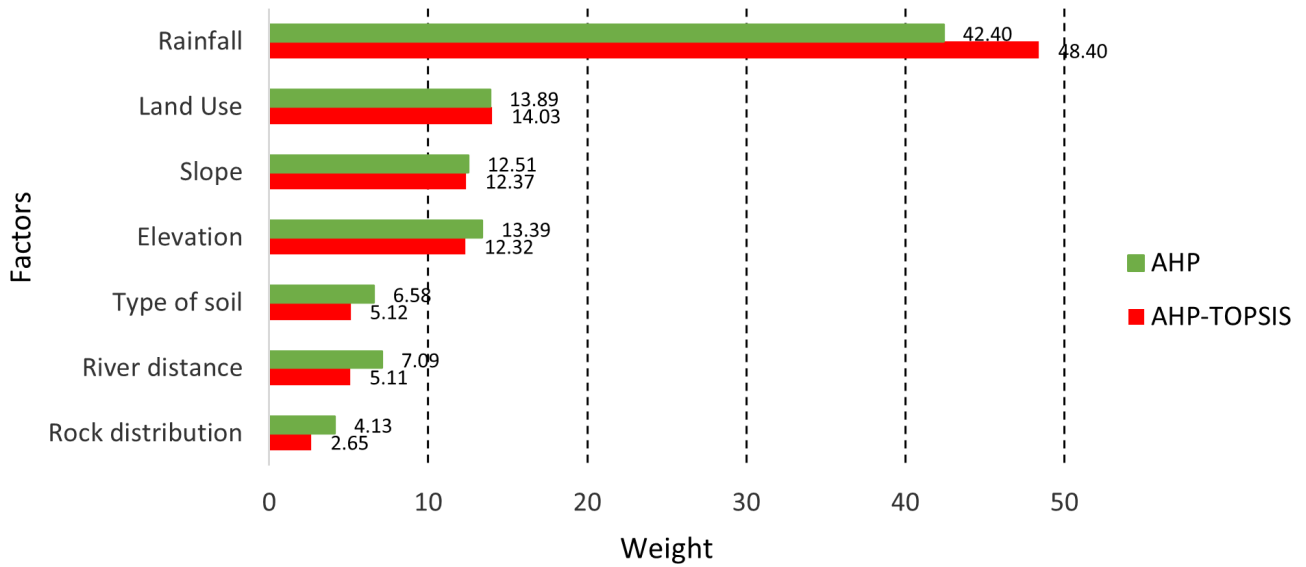


Figure 5 Graph of volcanic mudflow flood susceptibility factors

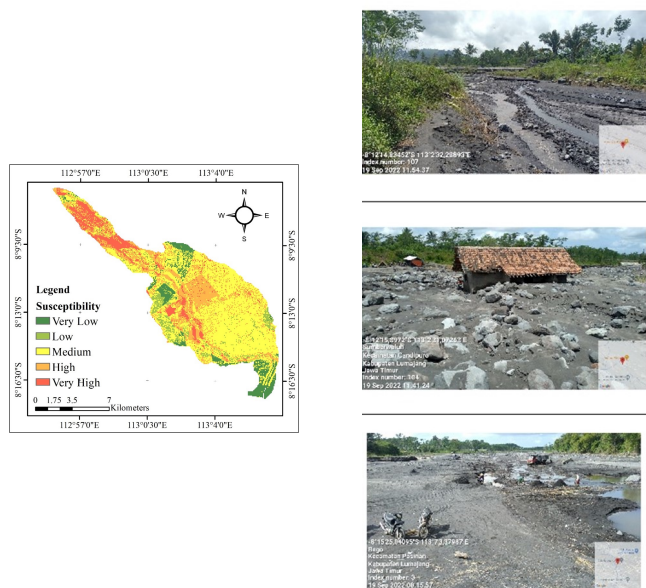


Figure 6 Volcanic mudflow flood susceptibility level map

### 5 DISCUSSIONS

The AHP method heavily depended on judgment and opinion of decision makers assigning subjective values to standards and alternatives, leading to potential biases and inconsistencies. Decision-makers could interpret and assess differently, possibly yielding different results (Kanani-Sadat et al., 2019). However, when AHP was paired with TOPSIS, susceptibility levels were influenced by both negative and positive factors within each

Table 5. Thickness of the volcanic mudflow deposit at the survey point

No.	Coordinate Point		Volcanic mudflow Deposits (m)	Susceptibility Rate
	X	Y		
1	723178.397	9096714.470	0.80	high
2	722594.111	9096306.779	2.00	very high
3	722527.921	9095659.590	1.80	very high
4	722699.426	9095342.865	2.80	very high
5	722916.863	9094773.216	2.50	very high
6	723496.677	909429.497	1.90	very high
7	723747.003	9094010.954	2.20	high
8	724136.540	9093250.903	0.80	high
9	724604.895	9092522.032	1.50	high
10	725582.940	9089926.918	1.60	very high

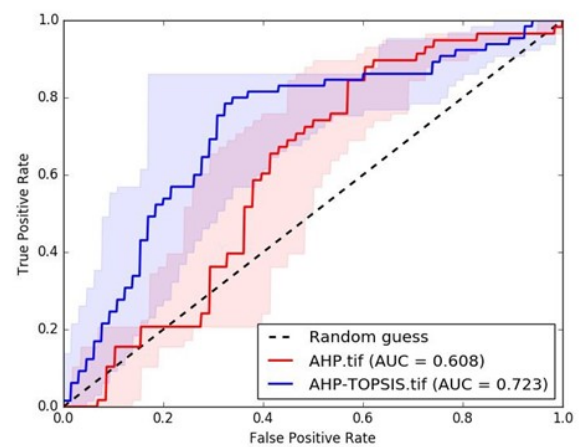


Figure 7 AUC validation result

area, with positive solutions representing the best performance for each criterion. This study found

rainfall to be the most influential factor in both AHP alone and its combination with TOPSIS due to its role in modulating volcanic activity (Farquharson and Amelung, 2020). The validation test showed that the AHP-TOPSIS combination was more accurate than AHP alone, suggesting it as a more effective method for modeling the mudflow flood susceptibility map (Pathan et al., 2022). Integrating TOPSIS with AHP reduced the influence of expert judgment, dealing with uncertainty through sensitivity analysis and thereby enhancing model accuracy (Menon and Ravi, 2022). Though AHP-TOPSIS proved successful, potential modifications to this multicriteria analysis were being considered, such as Fuzzy-TOPSIS, allowing for the aggregation of expert opinions without needing a consensus among them (Ziemba et al., 2020).

## 6 CONCLUSION

In conclusion, the occurrence of volcanic mudflow floods along the Rejali River, originating from Mount Semeru, has resulted in substantial property loss and disruptions to the local economy. The unique topography of the study area, characterized by flat terrain, presented challenges in effectively mapping the extent of volcanic mudflow floods. However, in this study, susceptibility modeling using the AHP-TOPSIS method effectively outlined the factors that influenced volcanic mudflow floods. This method aided in the development of mitigation strategies in response to eruptions from Mount Semeru. The AHP-TOPSIS method facilitated the estimation of flood potential in the area, and when combined with GIS, accurate mapping was achieved. This information played a crucial role in predictive actions and land use planning aimed at reducing the impact of floods caused by eruptions from Mount Semeru. In this study, two methods were employed to map volcanic mudflow flood susceptibility, both yielding high AUC validation results. The TOPSIS method effectively reduced the subjectivity inherent in the AHP method, identifying rainfall as the primary trigger for volcanic mudflow floods compared to other factors. Each method provided a more detailed analysis by leveraging the strengths of the respective techniques. Future studies should strive to enhance accuracy by incorporating DEM data with a higher resolution to generate more detailed maps.

## DISCLAIMER

The authors declare no conflict of interest.

## AVAILABILITY OF DATA AND MATERIALS

All data are available from the author.

## REFERENCES

- Akay, H. (2021), 'Flood hazards susceptibility mapping using statistical, fuzzy logic, and mcdm methods', *Soft Computing* **25**(14), 9325–9346.
- Armijon, Setyanto, Angin, G., Rahmadi, E. and Purba, A. (2018), 'Pemodelan analisis spasial aliran lahar dingin untuk mitigasi bencana gunung merapi', *Jurnal Geologi Sumber Daya Mineral* **1**, 105–112.
- Budiarti, W., Gravitiyani, E. and Mujiyo, M. (2018), 'Analisis aspek biofisik dalam penilaian kerawanan banjir di sub das samin provinsi jawa tengah', *Journal of Natural Resources and Environmental Management* **8**(1), 96–108.
- Ching-Lai Hwang, K. (1981), *Multiple Attribute Decision Making: Methods and Applications*, Springer-Verlag, New York.
- Costache, R., Țincu, R., Elkhrachy, I., Pham, Q. B., Popa, M. C., Diaconu, D. C., Avand, M., Costache, I., Arabameri, A. and Bui, D. T. (2020), 'New neural fuzzy-based machine learning ensemble for enhancing the prediction accuracy of flood susceptibility mapping', *Hydrological Sciences Journal* **65**(16), 2816–2837.
- Darmawan, K., Hani'ah, H. and Suprayogi, A. (2017), 'Analisis tingkat kerawanan banjir di kabupaten sampang menggunakan metode overlay dengan scoring berbasis sistem informasi geografis', *Jurnal Geodesi Undip* **6**(1), 31–40.
- Hariati, H., Wati, M. and Cahyono, B. (2018), 'Penerapan algoritma c4.5 pada penentuan penerima program bantuan pemerintah daerah di kabupaten kutai kartanegara', *Jurnal Rekayasa Teknologi Informasi (JURTI)* **2**(2), 106.
- Hidayah, E., Indarto, Lee, W.-K., Halik, G. and Pradhan, B. (2022), 'Assessing coastal flood sus-

ceptibility in east java, indonesia: Comparison of statistical bivariate and machine learning techniques', *Water* **14**(23), 1–18.

Irawan, I., Diara, I. and Bhayunagiri, I. (2019), 'Pemetaan potensi lokasi pengungsian akibat bencana letusan gunung agung di kabupaten karangasem berbasis sistem informasi geografis (sig)', *Journal of Tropical Agroecotechnology* **8**(4), 371–380.

Kanani-Sadat, Y. et al. (2019), 'A new approach to flood susceptibility assessment in data-scare and ungauged regions based on gis-based hybrid multi criteria decision-making method', *Journal of Hydrology* **572**, 17–31.

Khosravi, K. et al. (2018), 'A comparative assessment of decision trees algorithms for flash flood susceptibility modeling at haraz watershed, northern iran', *Science of the Total Environment* **627**, 744–755.

Khosravi, K. et al. (2019), 'A comparative assessment of flood susceptibility modeling using multicriteria decision-making analysis and machine learning methods', *Journal of Hydrology* **573**, 311–323.

Lappas, I. and Kallioras, A. (2019), 'Flood susceptibility assessment through gis-based multicriteria approach and analytical hierarchy process (ahp) in a river basin in central greece', *IRJET* pp. 738–751.

Larasati, Z. (2017), 'Pemetaan daerah risiko banjir lahar berbasis sistem informasi geografis untuk menunjang kegiatan mitigasi bencana (studi kasus: Gunung semeru, kabupaten lumajang', *Tugas Akhir* **4**, 9–15.

Menon, R. and Ravi, V. (2022), 'Using ahp-topsis methodologies in the selection of sustainable suppliers in an electronics supply chain', *Cleaner Materials* **5**(100130).

Meydani, A., Dehghanipour, A., Schoups, G. and Tajrishy, M. (2022), 'Daily reservoir inflow forecasting using weather forecast downscaling and rainfall-runoff modeling: Application to urmia lake basin, iran', *Journal of Hydrology: Regional Studies* **44**, 101228.

Nyimbili, P., Erden, T. and Karaman, H. (2018), 'Integration of gis, ahp and topsis for earthquake hazard analysis', *Natural Hazards* **92**(3), 1523–1546.

Oktavia, A. et al. (2022), 'Peran pemerintah dan organisasi non-pemerintah dalam rehabilitasi dan rekonstruksi pasca erupsi gunung semeru', **6**(4), 6937–6942.

Pathan, A. et al. (2022), 'Ahp and topsis based flood risk assessment- a case study of the navsari city, gujarat, india', *Environmental Monitoring and Assessment* **194**(509).

Pratiwi, E. (2020), 'Analisis tingkat kerawanan banjir di kabupaten lamongan', *Swara Bhumi* **3**(3), 1–9.

Purnawali, H. (2018), 'Flood vulnerabilty analysis at sidoarjo regency using geographic information system and remote sensing', p. 184.

Safitri, E., Hayati, N. and Bioresita, F. (2021), 'Analisis deformasi akibat aktivitas vulkanik menggunakan data citra sentinel-1a dan metode dinsar three-pass interferometry (studi kasus: Gunung semeru, jawa timur)', *Jurnal Teknik ITS* **10**(2).

Saputra, A., Santoso, D. and Ade Yudono, A. (2020), 'Zonasi tingkat kerawanan banjir pada ruas bekas sungai di kabupaten sukoharjo', *Jurnal Geografi* **12**(01), 255.

Seejata, K. et al. (2018), 'Assessment of flood hazard areas using analytical hierarchy process over the lower yom basin, sukhothai province', *Procedia Engineering* **212**, 340–347.

Ulfiana, D. (2020), 'Analisis kerawanan banjir sebagai pendukung perencanaan model water sensitive urban design di kabupaten klaten (peer review)'.

Ulfiana, D. and Sari, U. (2020), 'Analysis of flood risk to support sustainable development in the coastal area of semarang city', *Ruang* **6**(2), 102–111.

Ziemba, P., Becker, A. and Becker, J. (2020), 'A consensus measure of expert judgment in the fuzzy topsis method', *Symmetry* **12**(2), 204.

[This page is intentionally left blank]